Magnetic mentor

David Pratt
Tensor Research
E david.pratt@tensor-research.com.au

Depth of penetration

How far can we see beneath the magnetic basement surface? In general, it is less than you intuitively expect. **Figure 1** illustrates the concept of relative penetration depths beneath an unconformity surface that truncates a sequence of folded formations. Folded sequences beneath cover are common in Palaeozoic, Proterozoic and Archean terranes. Here, I am assuming that the overlying sediments are non-magnetic and the magnetic field anomalies are caused by formations within the basement.

Unconformity dominance

While there is no precise answer for penetration depth, I start by asserting that 90% of the magnetic anomaly is contributed by a thin slice through the top of the basement rocks. The thickness of this slice is equal to the magnetic sensor height above the unconformity. So, if the aircraft is flying at 100 m above the unconformity the depth of penetration is 100 m.

The magnetic rock properties of that 100 m slice dominate the amplitude and appearance of your magnetic images. The remaining 10% is contributed by rocks all the way to the Curie Depth where crustal rocks lose their magnetisation. The depth of penetration shrinks further for the first vertical derivative (1VD) where the penetration depth decreases to 50% or 50 m in this example.

This principle scales from just a few metres down to the Curie Depth. In mineral exploration, targeting depths are typically less than 1000 m, but the geological mapping objectives may still require an understanding of geology down to depths of 10 km or more because of their influence on structure, rock composition and fluid flow.

Testing the assertion

Figure 2 shows the computed TMI and 1VD anomalies (blue curves) for a 200 m wide vertical formation with the top unconformity truncation surface at 100 m below the sensor and extending to a depth of 10 000 m. The depth extent is changed to 1000 (green), 500 (orange) and 200 (red) m. The magnetic susceptibility is then inverted against the original 10 000 m model TMI and 1VD data and the inverted anomalies have the same colours as the models. You can see that the differences between the original model and inversion results are relatively small with the largest differences occuring on the flanks where they are more likely to be exposed to interference from nearby anomalies. I used the RMS mismatch in each case to estimate the relative contribution from each depth range. In this model, 92% of the contribution comes from the top 200 m for TMI and 94% for the 1VD data.

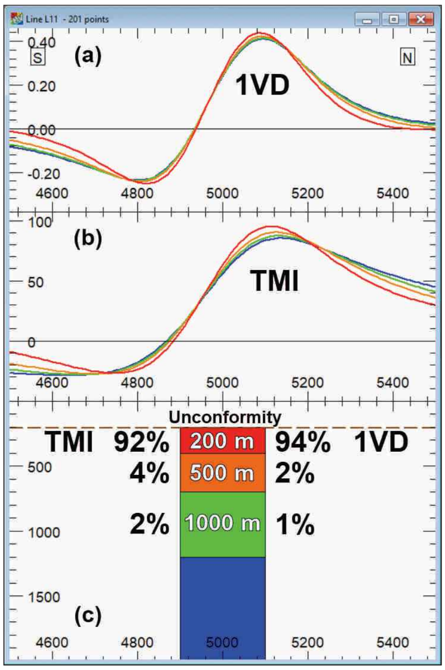

Figure 2. *1VD (a) and TMI (b) inversion curves for the green, orange and red formations after susceptibility inversion of the 10 000 m deep formation model (blue) data. The percentage contribution to the field response is shown beside each formation segment.*

An anomaly from a deeper formation must have a significantly higher susceptibility and depth separation for clear recognition in an image. The unconformity is the dominant contributing surface to the anomaly. This is the reason that a 1VD magnetic image is an excellent proxy for a magnetic lithology map of the upper basement surface.

Amadeus Basin examples

Figure 3(a) shows a coloured and shaded TMI image (linear stretch) from the Northern Territory, Amadeus Basin where the deepest units are believed to exceed 10 km. The basin sits mostly beneath the smoother parts of the image. Detailed

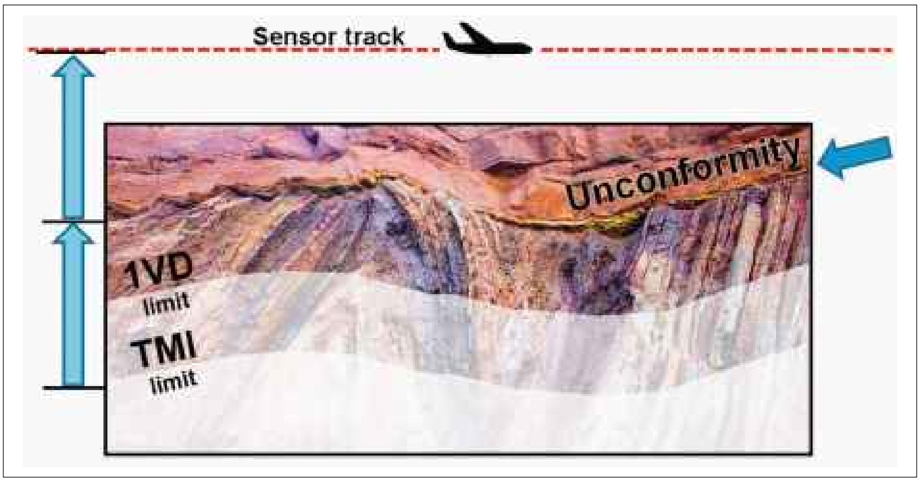

Figure 1. *A schematic view of the relative 90% penetration depth beneath a magnetic unconformity for the first vertical derivative (1VD) and the total magnetic intensity (TMI) relative to the height of the magnetic sensor above the unconformity.*

images from the north-east corner are used to illustrate the difference between depth of investigation (DI), depth of penetration (P) and outcrop (OC). The deep source basement anomalies are derived from a highly magnetic thick pre-Amadeus rift sequence of mafic igneous rocks. The southern margin of the basin appears to be overthrust by the Musgrave complex (P) where the high amplitude pre-Amadeus rift sequence anomalies can be seen through the thin, less magnetic Musgrave thrust sheet (red arrows).

Figure 3(b) is a monochrome TMI magnetic image subset from the rectangular area in (a). You can see a rapid change in depth of investigation from the highly magnetic northern Arunta Complex and a slowly deepening set of anomalies from the southern edge towards the north-west (blue arrow, DI 1). Note slightly smoother anomalies at the edge of the Arunta block (DI 2 blue arrow) where there is shallow cover against what is inferred to be a major structural boundary.

Figure 3(c) shows the separation of very low amplitude magnetic anomalies (green ellipse) within the basin sequence using a 5 km high pass FFT filter to reduce the amplitude of the deep high amplitude basement anomalies. The clipped linear range used in this filtered image is -1 to +1 nT compared with the clipped TMI range used in 3(b) of -500 to +500 nT and the total range of the data in 3(a) is ~9,000 nT. The Amadeus Basin sequence anticlines and synclines only begin to appear at very low thresholds due to the low susceptibilities of the associated sedimentary formations (Austin *et al*., 2017). The Walker Syncline (WS green ellipse) is a good example of penetration through the surface unconformity where the near surface anomalies are visible on much higher long wavelength anomalies from basement.

See the ***Magnetic mentor* series** link to download data and related information for this and previous columns.

Reference

Austin, J. R., S. Schmid and C.A. Foss. 2017. Using stratiform magnetic anomalies to map near-surface architecture: insights from the Amadeus Basin. *Australian Journal of Earth Sciences*, 64(3), 353–383. https://doi.org/10.1080/08120099.2017.1290683

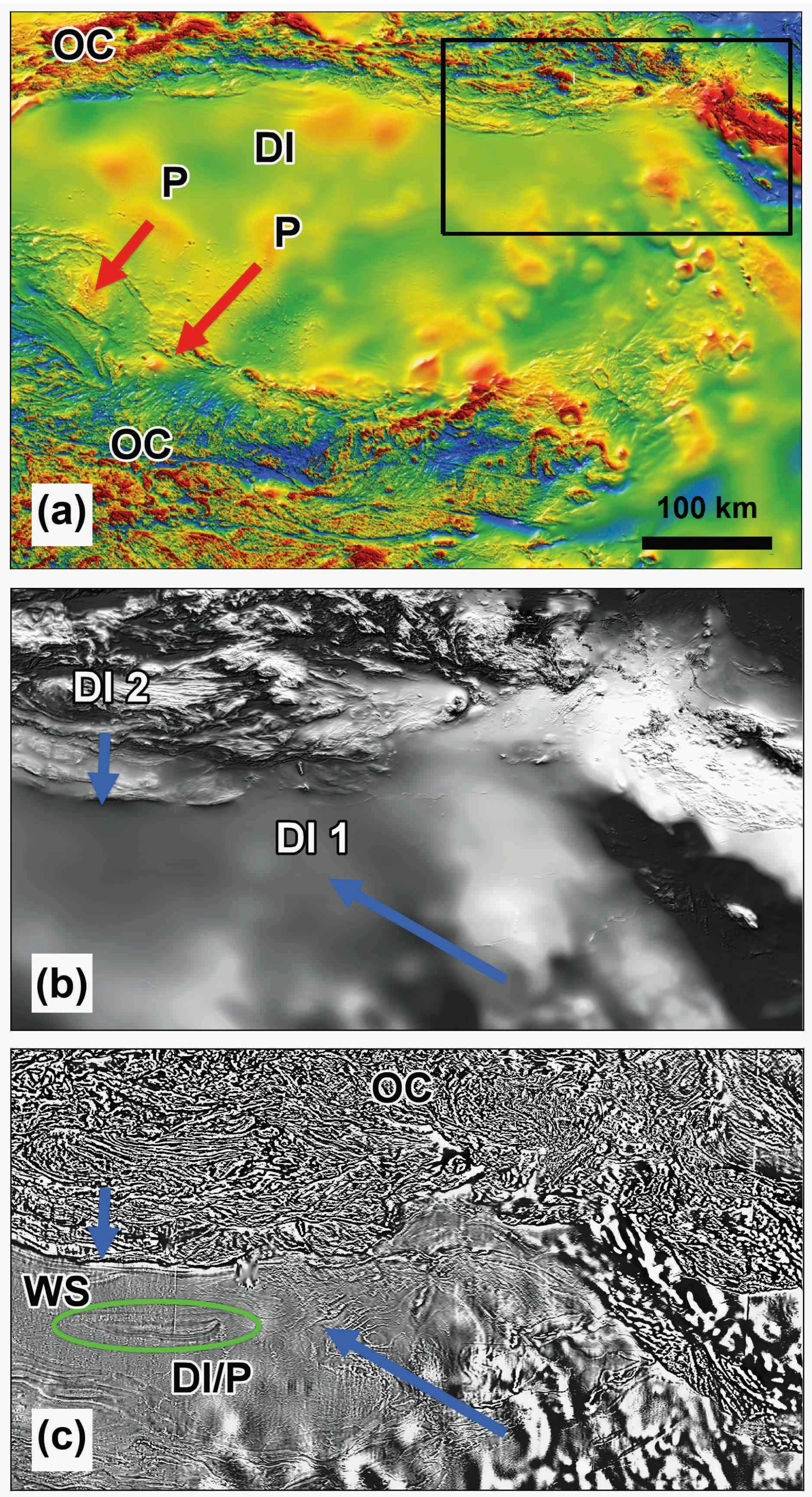

Figure 3. *Colour overview image (a) of the Arnhem Land, NT 400 m line spacing magnetic survey over the Amadeus Basin where the black rectangle shows the location of detailed images (b) and (c). Monochrome TMI image (b) with linear stretch. Monochrome image (c) of the +/-1 nT high pass filter (c). See text for image explanation.*